Title

Caspase-8 mutations in head and neck cancer confer resistance to death receptor-mediated apoptosis and enhance migration, invasion, and tumor growth

Journal

Molecular Oncology, 8(7)

ISSN

1574-7891

Authors

Li, Changyou
Egloff, Ann Marie
Sen, Malabika
et al.

Publication Date

2014-10-01

DOI

10.1016/j.molonc.2014.03.018

Peer reviewed

MOLECULAR ONCOLOGY 8 (2014) 1220–1230

available at www.sciencedirect.com

ScienceDirect

www.elsevier.com/locate/molonc

Caspase-8 mutations in head and neck cancer confer resistance to death receptor-mediated apoptosis and enhance migration, invasion, and tumor growth

Changyou Li[a], *Ann Marie Egloff*[b], *Malabika Sen*[b], *Jennifer R. Grandis*[b,c], *Daniel E. Johnson*[a,c,*]

[a]*Department of Medicine, University of Pittsburgh, University of Pittsburgh Cancer Institute, Pittsburgh, PA 15213, USA*

[b]*Department of Otolaryngology, University of Pittsburgh, University of Pittsburgh Cancer Institute, Pittsburgh, PA 15213, USA*

[c]*Department of Pharmacology & Chemical Biology, University of Pittsburgh, University of Pittsburgh Cancer Institute, Pittsburgh, PA 15213, USA*

ARTICLE INFO

Article history:
Received 17 December 2013
Received in revised form
11 March 2014
Accepted 26 March 2014
Available online 18 April 2014

Keywords:
Caspase-8
HNSCC
Extrinsic apoptosis
Migration
Invasion

ABSTRACT

Little is known regarding molecular markers in head and neck squamous cell carcinoma (HNSCC) that predict responsiveness to different therapeutic regimens or predict HNSCC progression. Mutations in procaspase-8 occur in 9% of HNSCC primary tumors, but the functional consequences of these mutations are poorly understood. In this study, we examined the impact of four, representative, HNSCC-associated procaspase-8 mutations on activation of the extrinsic apoptosis pathway, as well as cellular migration and invasion, and *in vivo* tumor growth. All four mutant proteins acted to potently inhibit activation of apoptosis following treatment with TRAIL or agonistic anti-Fas. In contrast to wild-type procaspase-8, the mutant proteins were not recruited to FADD following treatment with TRAIL or anti-Fas, but may be constitutively bound by FADD. Three of the four procaspase-8 mutants promoted enhanced cellular migration and invasion through matrigel, relative to that seen with the wild-type procaspase-8 protein. Procaspase-8 mutation also stimulated the growth of HNSCC xenograft tumors. These findings indicate that HNSCC-associated procaspase-8 mutations inhibit activation of the extrinsic apoptosis pathway and are likely to represent markers for resistance to therapeutic regimens incorporating death receptor activators. Moreover, procaspase-8 mutations may serve as markers of HNSCC tumor progression, as exemplified by enhanced migration, invasion, and tumor growth.

* *Corresponding author*. University of Pittsburgh School of Medicine, Room 2.18c, Hillman Cancer Center, 5117 Centre Avenue, Pittsburgh, PA 15213, USA. Tel.: +1 412 623 3245; fax: +1 412 623 7768.
E-mail address: johnsond@pitt.edu (D.E. Johnson).

1574-7891/$ – see front matter © 2014 Federation of European Biochemical Societies. Published by Elsevier B.V. All rights reserved.
http://dx.doi.org/10.1016/j.molonc.2014.03.018

1. Introduction

Head and neck squamous cell carcinoma (HNSCC), the 7th leading cause of cancer mortality worldwide, is most commonly detected as advanced locoregional disease at initial diagnosis (Jemal et al., 2009; Mehanna et al., 2010). Despite a treatment armamentarium of surgery, radiation, and chemotherapy (platinum- or taxane-based) for patients with advanced disease, roughly 50% of these individuals will recur within 5 years, and the overall 5-year survival rate is only 50–60% (Fung and Grandis, 2010). Complicating treatment efforts are the considerable toxicities and side effects associated with current standard of care. Patients treated with surgery, radiation, and/or chemotherapy typically suffer disfigurement, difficulties in swallowing and speaking, as well as other adverse toxicities (Fung and Grandis, 2010). Moreover, relatively little information is available about molecular markers that predict HNSCC progression or responsiveness/resistance to therapy, including the FDA-approved EGFR monoclonal antibody cetuximab (Bonner et al., 2010). Thus, endeavors to rationally stratify HNSCC patients for different therapeutic regimens have proven difficult. In this regard, recent sequencing of HNSCC tumors has sought to determine the mutational landscape in this disease, with the hope of identifying markers that would be useful for prognostication and patient stratification.

Stransky et al. (Stransky et al., 2011) and Agrawal et al. (Agrawal et al., 2011) reported whole exome sequencing of 74 and 32 HNSCC primary tumors, respectively. Sequences encoding procaspase-8 were found to be mutated in 7% of patients. Similarly, mutations in procaspase-8 coding sequences have been identified in 9% of HNSCC patients ($n = 310$ tumors) in The Cancer Genome Atlas (TCGA; mutation data obtained from the cBio portal (Cerami et al., 2012)). Genomic analysis has revealed that the procaspase-8 mutations occurring in HNSCC are associated with fewer total and focal copy number alterations, and commonly are found in conjunction with HRAS mutations (Pickering et al., 2013). However, the impact of HNSCC-associated procaspase-8 mutations on disease progression, and the mechanism of action of the mutant proteins, remain unknown.

Wild-type caspase-8 protein plays a key role in the extrinsic, or death receptor-mediated, apoptosis pathway (Fulda, 2009). The procaspase-8 zymogen consists of a prodomain containing two death effector domains (DEDa and DEDb), a large subunit, and a small subunit (Degterev et al., 2003; Zhao et al., 2010). Following stimulation of a cell surface death receptor, procaspase-8 is recruited to the death-inducing signaling complex (DISC) affixed to the cytoplasmic region of the receptor (Dickens et al., 2012; Martin et al., 1998; Muzio et al., 1998; Schleich et al., 2012; Yang et al., 1998). The recruited procaspase-8 then undergoes processing to yield active caspase-8, which subsequently cleaves and activates the executioner caspase, caspase-3. Thus, caspase-8 mediates activation of the extrinsic apoptosis pathway by ligands in the tumor necrosis factor (TNF) family of death ligands, including Fas ligand and TRAIL. In addition, in response to TNF, caspase-8 is involved in mediating activation of anti-apoptotic NF-κB (Chaudhary et al., 2000). Complexes of caspase-8 with FADD and c-FLIP$_L$ also act to inhibit RIPK-dependent necrosis (Oberst et al., 2011). More recently, non-protealytic functions of caspase-8 have been identified, including promotion of cell adhesion, motility, and metastasis of neuroblastoma and lung cancer cell lines via Src-mediated phosphorylation of Tyr380 (Barbero et al., 2008; Finlay and Vuori, 2007; Helfer et al., 2006; Senft et al., 2007; Stupack et al., 2006).

Mutation of procaspase-8 has also been reported in hepatocellular carcinoma (Soung et al., 2005b), gastric carcinoma (Soung et al., 2005a), and colorectal carcinoma specimens (Kim et al., 2003), suggesting an important consequence of these mutations for the growth or survival of these tumors. In HNSCC, an early report identified a frameshift mutation in procaspase-8 as producing a fusion protein antigen recognized by cytotoxic T lymphocytes (Mandruzzato et al., 1997). Ando et al. subsequently identified a missense procaspase-8 mutation (G325A) in a HNSCC cell line (T3M-1 CI-10) that activates NF-κB signaling to a greater degree than wild-type caspase-8 when exogenously expressed in cells (Ando et al., 2013). Pickering et al. have identified 7 HNSCC cell lines that harbor procaspase-8 mutations and report that these cell lines tend to be more tumorigenic in athymic mice than nonsyngenic HNSCC cell lines harboring wild-type procaspase-8 (Pickering et al., 2013).

In this study we sought to determine the impact of procaspase-8 mutations identified in primary HNSCC tumors on activation of the extrinsic apoptosis pathway, as well as cellular migration and invasion, and *in vivo* tumor growth. Expression of 4 representative procaspase-8 mutations profoundly inhibited caspase activation and cell death following treatment with TRAIL or agonistic anti-Fas antibody. The mutant proteins also differed from wild-type procaspase-8 in their recruitment to DISC components. We further determined that 3 of 4 mutants promoted cellular migration and invasion, and a selected mutant enhanced HNSCC xenograft tumor growth. Collectively, our findings provide experimental evidence that procaspase-8 mutations associated with HNSCC serve as markers of resistance to death ligands, and may have value in predicting locoregional invasion or distant metastasis in HNSCC.

2. Materials and methods

2.1. Cells and reagents

The human HNSCC cell lines UM-SCC-22A, UM-SCC-22B, UM-SCC-1, 1483, Cal33, UPCI:SCC090, UM-SCC-47, and UD-SCC-2 (Lin et al., 2007), and HeLa cells were maintained in DMEM containing 10% heat-inactivated fetal bovine serum (FBS) and 100 units/mL of penicillin/streptomycin (Gibco Life Technologies). Jurkat cells were cultured in RPMI 1640 supplemented with 10% FBS and antibiotics. Cell lines were genotypically validated using the AmpFLSTR Profiler Plus Amplification Kit (A&B Applied Biosystem). TRAIL was obtained from Peprotech (310-04). *Pfx*50™ DNA Polymerase (12355-012) and MAX Efficiency® DH5α™ Competent Cells

(18259-012) were from Invitrogen. Oligonucleotides were synthesized by Integrated DNA Technologies.

2.2. Generation of procaspase-8 mutant cell lines

The cDNAs encoding wild-type or mutant procaspase-8 proteins were inserted into the HindIII/BamHI polylinker sites of p3XFLAG-CMV-14 (Sigma). Plasmid pcDNA3-Casp8 (Addgene; 11817), encoding full-length wild-type procaspase-8, was used as a template for PCR generation of insert cDNAs. PCR reactions for all procaspase-8 cDNAs utilized the 5′ primer: 5′-GCAAGCTTGCCACCATGGACTTCAGCAGA-3′. The following reverse primers were used: 5′- GCGGATCCATCAGAAGGGAAGACAAGT-3′ (for wild-type and L105H mutant), 5′-GCGGATCCCCTTTCCATCTCCTCCTT-3′ (for E89*), 5′-GCGGATCCATCAGTCTCAACAGGTA-3′ (S375*), 5′-GCGGATCCTAAATCCATTTCTAAATAGG-3′ (S386*). Site-directed mutation of L105 to H105 utilized PCR-based mutagenesis, and the following internal primers covering the mutation site: 5′-TCTGATAGTGCATGACCCTGTAG-3′ (reverse) and 5′-CATGCACTATCAGATTTCAGAAG-3′ (forward). The expression construct pCR3.V64-Met-Flag-stop, encoding full-length c-FLIP$_L$, was provided by Hannah Rabinowich (Hou et al., 2010). All constructs were verified by restriction enzyme and sequence analysis. Constructs (40 μg) were transfected into HeLa or UM-SCC-47 using Lipofectamine 2000 Reagent (Invitrogen). 48-hours after transfection, cells were selected in G418-containing medium (1 mg/mL). Following selection for 2 weeks in G418, single clones were isolated, and expression of the mutant proteins verified by immunoblotting. All experiments utilized independent clonal cell lines.

2.3. Immunoblotting and co-immunoprecipitations

Immunoblotting was performed as previously described (Li and Johnson, 2013). Antibodies used were: anti-caspase-8 (BD Pharmingen; #551242), anti-FADD (Santa Cruz Biotechnology, Inc.; sc-5559), anti-PARP (Cell Signaling Technology; 9542s), anti-caspase-3 (ENZO Life Sciences; Adl-aap-113); anti-β-actin and anti-Flag (Sigma; A5441 and F3165, respectively), anti-Fas (Millipore; 05-201). For co-immunoprecipitation experiments cells were plated at 2×10^6 cells per 10 cm dish, then treated for 2 h with TRAIL (500 ng/mL), agonistic anti-Fas (1 μg/mL), or control PBS. Following treatement, cells were detached by scaping and lysed in DISC IP buffer (10 mmol/l Tris, pH 7.5, 150 mmol/l NaCl, 10% glycerol, 1 mmol/L EDTA, 1% Triton X-100) containing protease inhibitor cocktail (1 tablet/10 mL; Roche Applied Sciences). Dynabeads protein A (Invitrogen) were rinsed 3 times with DISC IP buffer using a DyNAMag-Spin Magnetic Particle Concentrator (Invitrogen) magnetic particle concentrator. Cell lysates (500 μg) were precleared by incubation with 20 μl of beads overnight at 4 °C. Beads were then removed and the precleared lysates were incubated with 20 μl of rabbit anti-FADD at 4 °C overnight. Washed Dynabeads protein A (20 μl) were then added to each tube and incubated for 4 h at 4 °C. After 3 washes in DISC IP buffer, bead-antibody complexes were resuspended in 50 μl of loading buffer, boiled for 10 min, then placed on the magnet for 2 min. Supernatants were subjected to electrophoresis on SDS/PAGE gels, followed by immunoblotting. In the case of anti-Flag immunoprecipitations, precleared cell lysates were incubated with 2 μl anti-Flag mouse monoclonal antibody, followed by purification of the immune complexes using the Dynabeads protein A.

2.4. Viability, apoptosis, and colony formation assays

The IC_{50}'s of cell lines for TRAIL or anti-Fas were determined by MTT assays. Prior to treatment, HeLa and transfected HeLa cells were plated at 3500 cells/well in 96-well plates. UM-SCC-1, Cal33, UM-SCC-47 and transfected UM-SCC-47 cells were plated at 3000 cells/well; 1483 and UPCI:SCC090 were plated at 4000 cells/well; UM-SCC-22A were plated at 6000 cells/well. Plated cells were allowed to recover overnight before treatment for 96 h and performance of MTT assays. For determination of cell viabilities, trypan blue exclusion assays were performed. Briefly, 2×10^6 cells/well were plated in triplicate in 6-well plates. After overnight recovery, cells were treated with TRAIL for 48 h. Treated cells were detached from plates by trypsinization and floating and detached cells were combined. A minimum of 300 cells counted per datapoint. For determination of Annexin V externalization, cells were treated with TRAIL for 48 h, followed by assessment using FITC Annexin V Apoptosis Detection kits (BD Pharmingen) and flow cytometric analyses. For colony formation assays, cells were plated at 2.5×10^5 cells per well in 6-well plates and allowed to grow for 24 h. The cells were then treated for 4 h with 500 nmol/L TRAIL, followed by detachment from the plates. The cells were replated in 6-well plates at 1000 cells/well, and allowed to grow for 10–14 days. Colonies were stained for 30 min with 0.5% crystal violet in 6% glutaraldehyde, then washed repeatedly with water. Colonies composed of >50 cells were counted.

2.5. Migration and invasion assays, and generation of xenograft tumors

Cell migration was assessed using wound-healing scratch assays. Cells were plated at 8×10^5 cells/well in 6-well plates and allowed to grow until 90–95% confluence was reached. Cells were then washed in PBS. The medium was then replaced with serum-free medium and the cells grown for an additional 24 h. Scratches were then made using a p200 pipette tip. Three independent images were then taken of each well at 0, 24, and 48 h timepoints. The wound gap distance was determined by measurement of photographic images. For invasion assays, 1.3×10^4 cells were inoculated into the top chamber of BD BioCoat GRF Matrigel invasion inserts (BD Biosciences) containing matrigel-coated filters in DMEM medium containing 0.2% FBS. The bottom chambers contained DMEM with 20% FBS. Cells were then incubated for 24 h, followed by three washes with PBS. Cotton swabs were used to remove noninvading cells from the upper chamber, prior to fixation with 2% paraformaldehyde. Filters were then stained with DAPI in VECTASHIELD mounting medium (Vector Laboratories, Inc.). Invading cells were counted by fluorescence microscopy, with five random fields counted. For generation of xenograft tumors, female athymic nude mice nu/nu (4–6 weeks old; Harlan Sprague–Dawley) were inoculated into the right and left flanks

(5 mice/group) with UM-SCC-47 harboring empty vector, or vector encoding wild-type procaspase-8 or the L105H procaspase-8 mutant (3×10^6 cells/inoculation). Once palpable, tumors were measured thrice/week. Mice were sacrificed and tumors harvested on day 28. Animal care was in strict compliance with University of Pittsburgh institutional guidelines, the Guide for the Care and Use of Laboratory Animals (National Academy of Sciences, 1996) and the Association for Assessment and Accreditation of Laboratory Animal Care International.

2.6. Statistical analysis

For comparison of two groups, student's *t*-test was applied. For comparison of multiple groups, one-way ANOVA, followed by student's Neuman-Keul's test was used to determine statistical significance. Statistical comparison of tumor volumes was performed using a nonparametric Mann–Whitney two-tailed test. All data were analyzed by Prism software (version 4; Graphpad Software, Inc.).

3. Results

3.1. Procaspase-8 mutants fail to undergo processing in response to TRAIL

We recently reported whole exome sequencing of a cohort of 74 patients with HNSCC (Stransky et al., 2011). Mutations in the procaspase-8 coding region were identified in 5 patients, and a splice site mutation identified in a sixth patient. The locations of the coding mutations are depicted in Figure 1A, with a missense mutation (L105H) occurring in the second death effector domain (DEDb), and nonsense mutations occurring in the linker between DEDa and DEDb (E89*), the linker between the large (p18) and small (p10) subunits (S375*), and near the beginning of the small subunit (S386*). The S386* mutation was observed in two different patients. A similar rate of HNSCC procaspase-8 mutation was reported by others (Agrawal et al., 2011). Moreover, sequencing of 310 HNSCC patient tumors by the TCGA has subsequently determined that 9% harbor procaspase-8 mutations (Cerami et al., 2012).

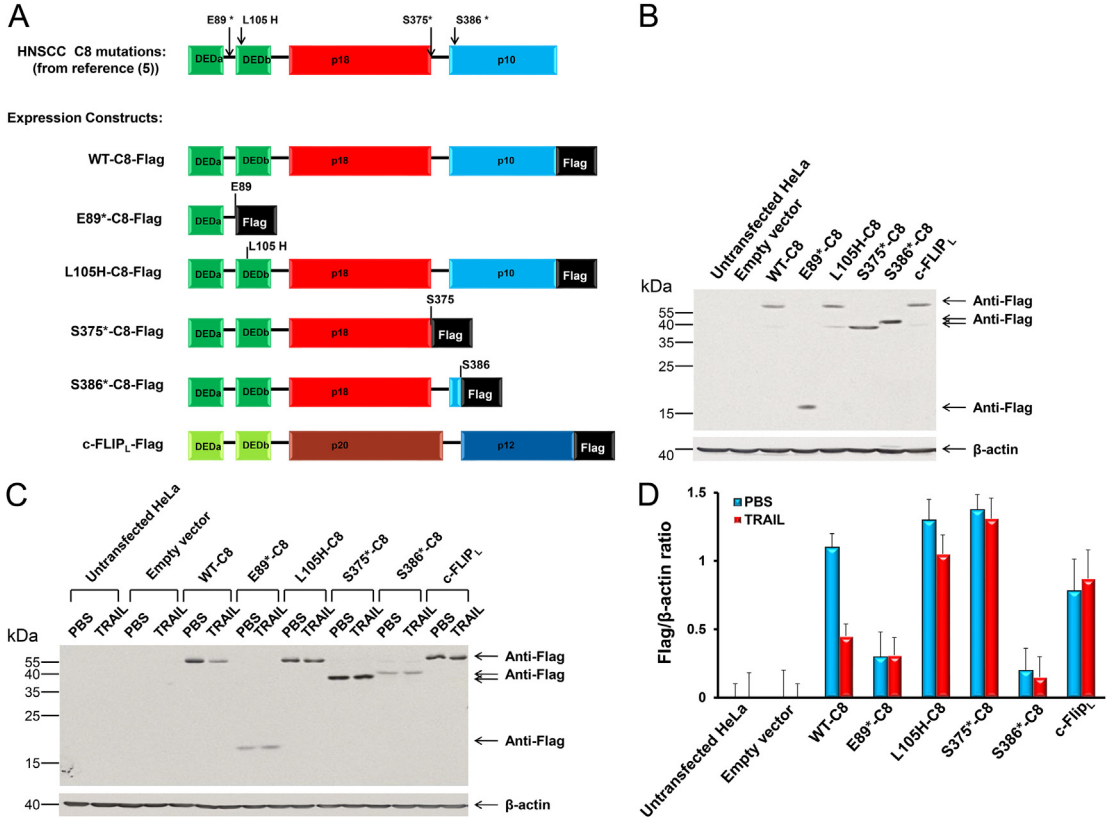

Figure 1 – Mutant procaspase-8 proteins fail to undergo processing in response to TRAIL treatment. (A) Schematic representation of HNSCC-associated missense and nonsense mutations in procaspase-8 (Stransky et al., 2011) and Flag-tagged mutant constructs. (B) HeLa cells were stably transfected with p3XFLAG-CMV-14 empty vector, or constructs encoding Flag-tagged wild-type or mutant procaspase, or c-FLIP$_L$. Following the isolation of single clones, whole cell lysates were prepared and subjected to immunoblotting with anti-Flag. Immunoblotting for β-actin was used to control for protein loading. Similar results were seen in 3 independent experiments. (C) Untransfected HeLa cells, or clonal transfected HeLa cells expressing empty vector or the indicated proteins were treated for 48 h with 500 ng/mL TRAIL (in PBS). Treatment with PBS in complete media was used as control. Following treatment, cells were subjected to immunoblotting with anti-Flag or anti-β-actin. (D) The data presented in panel C were quantified by densitometry and the ratio of Flag signal to β-actin signal determined in the control-treated (PBS) and TRAIL-treated cells.

To elucidate the functions of the procaspase-8 mutations identified in HNSCC, we generated epitope-tagged (Flag epitope) versions of the four mutations shown in Figure 1A for expression in human cells. As controls, we also generated Flag-tagged versions of wild-type procaspase-8 and c-FLIP$_L$. The c-FLIP$_L$ protein bears considerable homology to procaspase-8, but lacks catalytic activity (Irmler et al., 1997). Expression of c-FLIP$_L$ has been shown to inhibit death receptor-mediated activation of the extrinsic apoptosis pathway (Irmler et al., 1997). We first transfected expression constructs encoding the Flag-tagged proteins into HeLa cells, which are sensitive to the death ligand TRAIL or agonistic anti-Fas. Following isolation of clonal transfected cell lines, immunoblotting with anti-Flag was used to verify expression of the exogenous proteins (Figure 1B). As expected, the L105H mutant and c-FLIP$_L$ co-migrated with full-length, wild-type procaspase-8, while the E89*, S375*, and S386* truncation mutants migrated as smaller proteins. We then asked whether the procaspase-8 mutants undergo processing following treatment with TRAIL. As shown in Figures 1C and D, the levels of the wild-type procaspase-8 protein were markedly reduced after 48 h of TRAIL treatment, demonstrating that the Flag epitope did not disrupt procaspase-8 processing. However, in contrast to the wild-type protein, the cellular levels of the four procaspase-8 mutants, as well as c-FLIP$_L$, did not appreciably change in response to TRAIL treatment. These results indicate that the procaspase-8 mutants do not undergo processing following death receptor stimulation.

3.2. *Procaspase-8 mutants inhibit death receptor-mediated apoptosis in HeLa cells*

We next sought to determine the impact of the procaspase-8 mutant proteins on activation and propagation of the endogenous extrinsic apoptosis pathway. Cells were treated with TRAIL, followed by immunoblotting for endogenous caspase-8 (Figure 2A). Treatment of positive control Jurkat T leukemia cells led to loss of the 53/51 kDa procaspase-8 protein and appearance of the expected 43/41 kDa processed forms. Similarly, processing of endogenous procaspase-8 to the p43/p41 forms was easily detected following TRAIL treatment of untransfected HeLa cells, HeLa cells harboring empty vector, or HeLa cells expressing the Flag-tagged, wild-type procaspase-8 protein (Figure 2A). In addition, TRAIL treatment of these cell lines led to the appearance of processed caspase-3 and cleaved PARP protein, demonstrating efficient activation and propagation of the extrinsic apoptosis pathway (Figure 2A). By contrast, TRAIL treatment of cells expressing the Flag-tagged mutant procaspase-8 proteins, or Flag-tagged c-FLIP$_L$, failed to yield any detectable processing of the endogenous procaspase-8 or procaspase-3 proteins, or PARP cleavage. These results indicated that the mutant procaspase-8 proteins blocked TRAIL activation of the extrinsic apoptosis pathway.

To confirm the inhibitory impact of the procaspase-8 mutants on TRAIL-induced apoptosis, we assessed apoptosis induction by flow cytometric detection of Annexin V staining (Figure 2B). Cells expressing the mutant procaspase-8 proteins, or c-FLIP$_L$, demonstrated markedly reduced Annexin V staining following TRAIL treatment, relative to that seen in cells expressing the wild-type procaspase-8 protein or empty vector. Similarly, cells expressing the mutant procaspase-8 proteins demonstrated enhanced resistance to TRAIL in trypan blue exclusion assays (Figure 2C) and clonogenic survival assays (Figure 2D).

To quantitatively determine the degree of resistance to death receptor-mediated cell death conferred by the procaspase-8 mutants, cells were treated with varying concentrations of TRAIL or agonistic anti-Fas, followed by determination of IC$_{50}$ values (Table 1). Untransfected HeLa cells and HeLa cells harboring empty vector displayed highly similar sensitivities to both TRAIL and anti-Fas. Cells expressing the Flag-tagged wild-type procaspase-8 protein were roughly 3-fold more sensitive to TRAIL and anti-Fas, consistent with the pro-apoptotic activity of the wild-type protein. By contrast, cells expressing c-FLIP$_L$ displayed marked resistance to TRAIL and anti-Fas. Importantly, cells expressing the mutant procaspase-8 proteins also exhibited considerable resistance to TRAIL and anti-Fas. The lowest degree of resistance was shown by the smallest truncation mutant, E89*, which was 3.1- and 3.6-fold more resistant to TRAIL and anti-Fas, respectively, relative to vector-transfected HeLa cells. The L105H procaspase-8 mutant conferred the highest degree of resistance: greater than 11.5- and 5.9-fold resistance to TRAIL and anti-Fas, respectively. Collectively, our results demonstrate that the procaspase-8 mutant proteins inhibit activation of the extrinsic apoptosis pathway and ultimate cell death following stimulation of cell surface death receptors.

3.3. *Procaspase-8 mutants inhibit activation of the extrinsic apoptosis pathway in UM-SCC-47 HNSCC cells*

We next asked whether the procaspase-8 mutant proteins would act to inhibit death receptor-mediated cell death in the context of HNSCC cells. A panel of 7 HNSCC cells lines was first screened for responsiveness to either TRAIL or anti-Fas, by assessing processing/cleavage of endogenous procaspase-8, caspase-3, and PARP proteins (Supplementary Figures S1A & SB), and by determination of IC$_{50}$ values (Supplementary Table 1). Only one HNSCC cell line, UM-SCC-47, was shown to activate the extrinsic apoptosis pathway. Therefore, UM-SCC-47 cells were stably transfected with the constructs encoding the Flag-tagged wild-type or mutant procaspase-8 proteins, and immunoblotting with anti-Flag was used to verify expression of the proteins (Figure 2E). As shown in Figure 2F, UM-SCC-47 cells expressing the mutant procaspase-8 proteins, similar to HeLa cells expressing the mutant proteins, did not exhibit processing/cleavage of endogenous caspase-8, caspase-3, or PARP protein following treatment with TRAIL. UM-SCC-47 cells expressing the procaspase-8 mutants also displayed higher IC$_{50}$ values for TRAIL, relative to vector-transfected UM-SCC-47 cells (roughly 2–3 fold; Table 2). Thus, the mutant procaspase-8 proteins conferred resistance to death receptor-mediated apoptosis in UM-SCC-47 HNSCC cells, as well as in the HeLa cervical carcinoma cells.

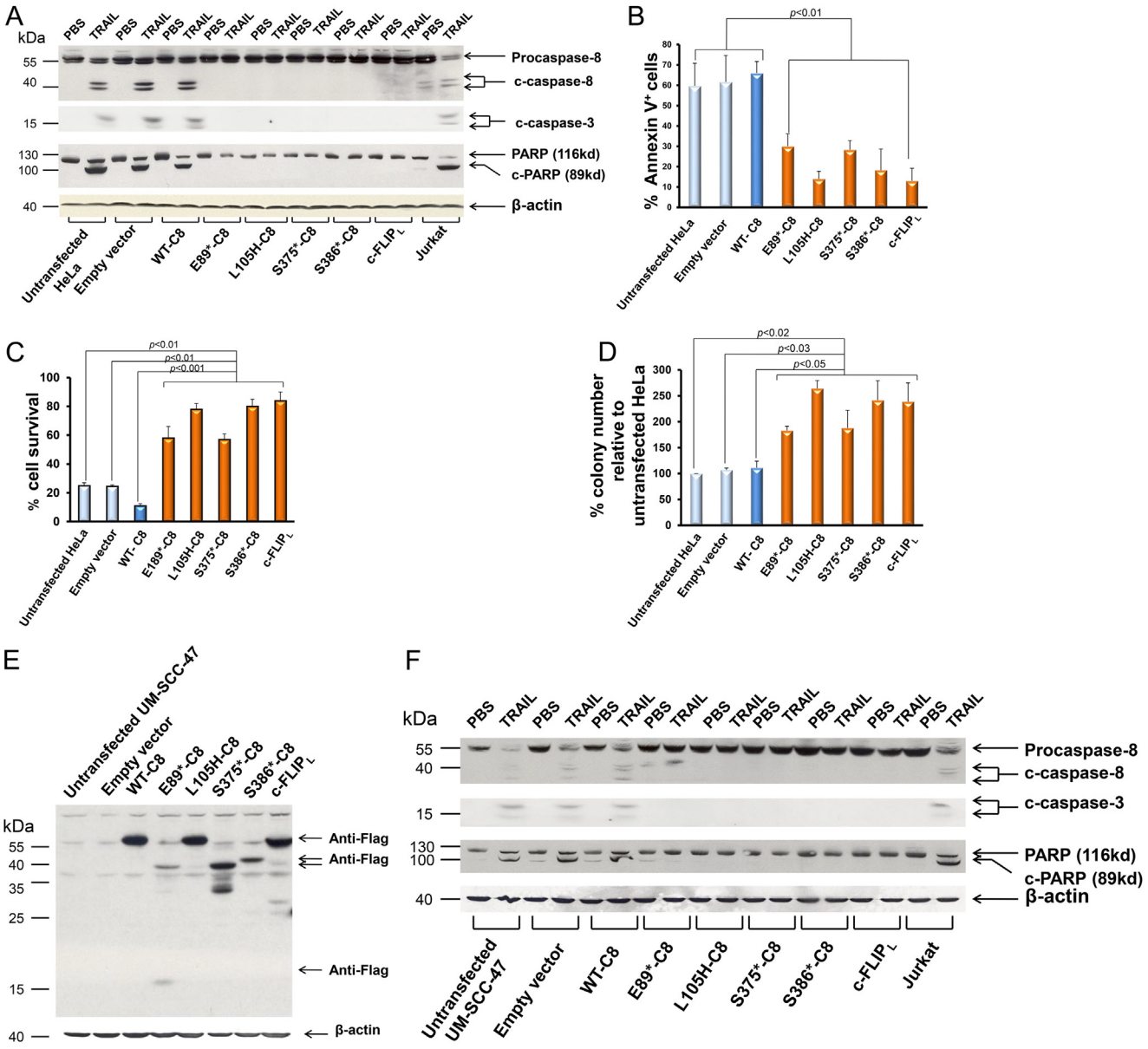

Figure 2 – Procaspase-8 mutant proteins inhibit TRAIL-induced cell death and activation of the extrinsic apoptosis pathway in HeLa cells and UM-SCC-47 HNSCC cells. (A) HeLa expressing exogenous wild-type or mutant procaspase-8, or c-FLIP$_L$ were treated in the absence (PBS diluent) or presence of 500 ng/mL TRAIL for 48 h. Whole cell lysates were subjected to immunoblotting for endogenous caspase-8, caspase-3, or PARP proteins. The locations of the caspase-8, caspase-3, and PARP full-length proteins and cleavage (c) products are indicated. Untransfected Jurkat T-leukemia cells were used as a positive control. Similar results were seen in 3 experiments. (B) HeLa cells expressing the indicated proteins were treated for 48 h with 500 ng/mL TRAIL followed by flow cytometric analysis of Annexin V staining. Columns represent the average percentage of Annexin V-positive cells from 3 independent experiments; error bars represent the SEM. (C) HeLa cells expressing the indicated proteins were treated for 48 h with 500 ng/mL TRAIL, followed performance of trypan blue exclusion assays. Columns represent the means from 3 independent experiments; error bars represent the SEM. (D) HeLa cells expressing the indicated proteins were treated for 4 h with 500 ng/mL TRAIL, followed by performance of colony formation assays. Data are graphed as the percentage of colonies relative to that seen with untransfected HeLa cells. Columns represent means from 3 independent experiments, and error bars the SEM. (E) UM-SCC-47 cells were stably transfected with empty vector, or constructs encoding Flag-tagged wild-type or mutant procaspase, or c-FLIP$_L$. Following the isolation of single clones, cells were subjected to immunoblotting with anti-Flag or anti-β-actin. (F) UM-SCC-47 cells expressing the indicated proteins were treated in the absence (PBS) or presence of 200 ng/mL TRAIL for 48 h. After treatment, cells were subjected to immunoblotting for endogenous caspase-8, caspase-3, or PARP. Representative results from 3 independent experiments are shown.

Table 1 – IC_{50}'s (96 h).

Cells	TRAIL	anti-Fas
HeLa	0.079 μg/mL	1.884 μg/mL
Empty vector	0.087 μg/mL	1.349 μg/mL
WT-C8	0.030 μg/mL	0.571 μg/mL
E89*-C8	0.267 μg/mL	4.799 μg/mL
L105H–C8	1 μg/mL	8 μg/mL
S375*-C8	0.436 μg/mL	5.435 μg/mL
S386*-CH	0.739 μg/mL	5.567 μg/mL
c-$FLIP_L$	1 μg/mL	8 μg/mL
Jurkat	0.01 μg/mL	0.0079 μg/mL

Table 2 – IC_{50}'s (96 h).

Cells	TRAIL
UM-SCC-47	0.036 μg/mL
Empty vector	0.032 μg/mL
WT-C8	0.031 μg/mL
E89*-C8	0.066 μg/mL
L105H–C8	0.098 μg/mL
S375*-C8	0.061 μg/mL
S386*-C8	0.079 μg/mL
c-$FLIP_L$	0.14 μg/mL

3.4. *Wild-type procaspase-8 proteins, but not procaspase-8 mutants are recruited to FADD during death receptor-mediated apoptosis*

Following engagement of the TRAIL and Fas death receptors, the adaptor protein FADD is recruited via its death domain (DD) to the cytoplasmic region of the oligomerized receptors, beginning formation of the death-inducing signaling complex (DISC). A death effector domain (DED) in FADD then serves as a recruitment site for the DEDa domain in the prodomain of procaspase-8 (Zhao et al., 2010). To determine whether the mutant procaspase-8 proteins are recruited to FADD following treatment with TRAIL or anti-Fas, we performed co-immunoprecipitation experiments of endogenous FADD and the Flag-tagged proteins (Figure 3A and B). Immunoprecipitation with anti-Flag, followed by immunoblotting with anti-FADD revealed elevated binding of wild-type procaspase-8 protein to FADD following TRAIL or anti-Fas treatment (Figure 3A). Similar results were obtained when lysates were first subjected to immunoprecipitation with anti-FADD followed by immunoblotting with anti-Flag (Figure 3B). By contrast, treatment with TRAIL or anti-Fas did not result in enhanced binding of the mutant procaspase-8 proteins to FADD. In the case of the L105H, S375*, and S386* mutants, however, it appears possible that the proteins are constitutively associated with FADD in the absence of death receptor stimulation.

3.5. *Cellular migration and invasion, and in vivo tumor growth, is enhanced by procaspase-8 mutants*

Recent studies have indicated that wild-type procaspase-8 protein may promote cell motility, and that this action is independent of any caspase-8 proteolytic activity (Frisch, 2008; Helfer et al., 2006; Senft et al., 2007; Torres et al., 2010). We examined the impact of the procaspase-8 mutant proteins on migration and invasion in HeLa and UM-SCC-47. Cellular migration was assessed using wound healing scratch assays by measuring wound (gap) width at 24 and 48 h, relative to gap width at $T = 0$ h (primary data shown in Supplementary Figures S2 & S3). As shown in Figure 4A, HeLa cells expressing the L105H, S375*, and S386* mutant procaspase-8 proteins demonstrated enhanced migration relative to cells engineered to express the wild-type procaspase-8 protein. The E89* mutant did not promote enhanced migration. Cells expressing the L105H procaspase-8 mutant exhibited particularly dramatic migration. We then examined the migration of UM-SCC-47 cells expressing either wild-type procaspase-8 or the L105H mutant (Figure 4B). Again, the L105H mutant promoted more rapid migration than the wild-type protein.

The invasive capacity of cells expressing the wild-type or mutant procaspase-8 proteins was then assessed by examining invasion across matrigel-coated filters following a gradient from 0.2% FBS to 20% FBS (representative primary data shown in Supplementary Figures S4 & S5). Figure 4C shows that 3 of the 4 mutants promoted enhanced invasiveness in HeLa. Only the E89* short truncation mutant did not. In UM-SCC-47 cells we confirmed enhanced invasion of cells expressing the L105H mutation (Figure 4D). Collectively, these findings show that 3 of the 4 procaspase-8 mutants identified in HNSCC patients can act to promote both migration and invasion through matrigel.

When next examined the impact of the L105H procaspase-8 mutant on HNSCC xenograft tumor growth. Nude mice were injected with UM-SCC-47 cells harboring empty vector, or vector encoding wild-type or L105H mutant procaspase-8, followed by assessment of tumor growth (Figure 4E). Although more tumors were detected in the wild-type group ($n = 8$) than the L105H mutant group ($n = 3$ tumors), the tumors from the wild-type group demonstrated very little growth by day 28. By contrast, the tumors arising in the L105H mutant procaspase-8 group exhibited rapid growth. Immunoblotting with anti-Flag verified expression of the epitope-tagged wild-type or L105H mutant proteins in tumors harvested on day 28 (Supplementary Figure S6).

3.6. *The E89* procaspase-8 truncation mutant exhibits reduced stability*

The E89* procaspase-8 mutant was the least potent among the procaspase-8 mutant proteins at inhibiting TRAIL- and anti-Fas-induced apoptosis (Table 1). Additionally, the E89* mutant, in contrast to the other procaspase-8 mutants, did not affect cellular migration or invasion (Figures 4A and C). Therefore, we examined the stability of the E89* mutant protein in comparison with wild-type procaspase-8 or the L105H procaspase-8 mutant. The addition of cycloheximide to cells led to rapid reduction of E89* levels, beginning 1–2 h after treatment (Supplemental Figure S7). By contrast, cycloheximide treatment did not substantially impact the levels of wild-type procaspase-8 or the L105H mutant. These findings indicate that the E89* truncation mutant has reduced stability

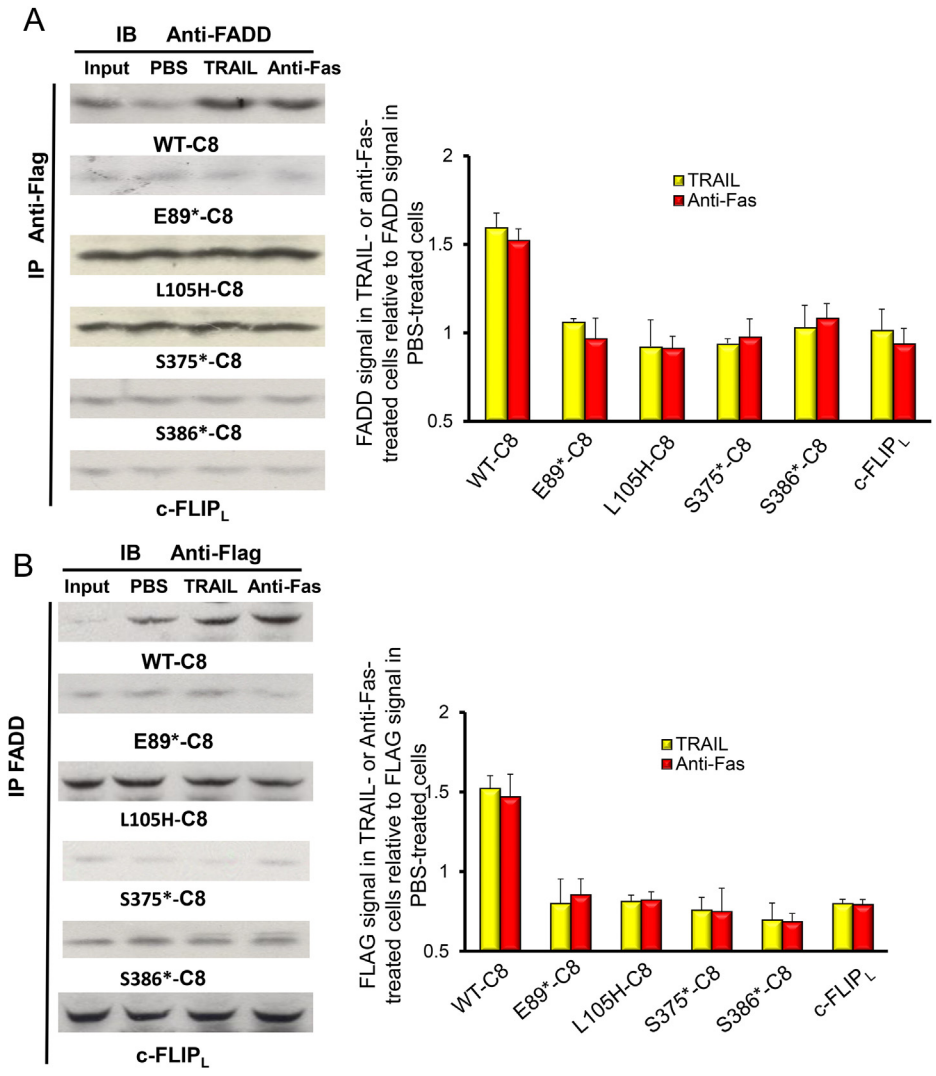

Figure 3 – Wild-type procaspase-8, but not mutant procaspase-8 proteins, is recruited to FADD during death receptor-mediated apoptosis. (A) Cells expressing Flag-tagged wild-type or mutant procaspase-8, or Flag-tagged c-FLIP$_L$ were treated for 2 h in the absence (PBS) or presence or TRAIL (500 ng/mL), or agonistic anti-Fas (1 μg/mL). Cells were then subjected to immunoprecipitation with anti-Flag antibody, followed by immunoblotting with anti-FADD. In the right hand panel densitometry was used to quantify the ratio of the Flag signal in treated versus control cells. Columns represent the means from 3 independent experiments, and error bars the SEM. Only the wild-type procaspase-8 protein demonstrated recruitment to FADD following death receptor stimulation. (B) Cells were treated as in panel A, followed by immunoprecipitation with anti-FADD and immunoblotting with anti-Flag. The ratio of the FADD signal in treated versus control cells was determined and graphed as in panel A.

in cells, which may contribute to the reduced biological activity of this mutant.

4. Discussion

HNSCC is a devastating disease with a high mortality rate. Among the most commonly mutated genes in HNSCC tumors is the gene encoding procaspase-8 (Agrawal et al., 2011; Stransky et al., 2011). In view of the critical role that caspase-8 is known to play in activation of the extrinsic apoptosis pathway, we set out to determine the impact of HNSCC-associated procaspase-8 mutations on apoptosis activation following death receptor stimulation. The four procaspase-8 mutations we tested involved alterations in different regions of the zymogen molecule, including truncations in the prodomain and catalytic subunits, as well as a missense mutation in the prodomain. All four procaspase-8 mutations were found to potently inhibit caspase activation and apoptotic cell death following treatment of cells with TRAIL or agonistic anti-Fas. These findings indicate that HNSCC tumors harboring procaspase-8 mutations are unlikely to be highly responsive to biological therapies based on death receptor ligands or agonists. Whether procaspase-8 mutation, and associated resistance to death ligands, plays an important role in the early development of HNSCC tumors is currently unknown.

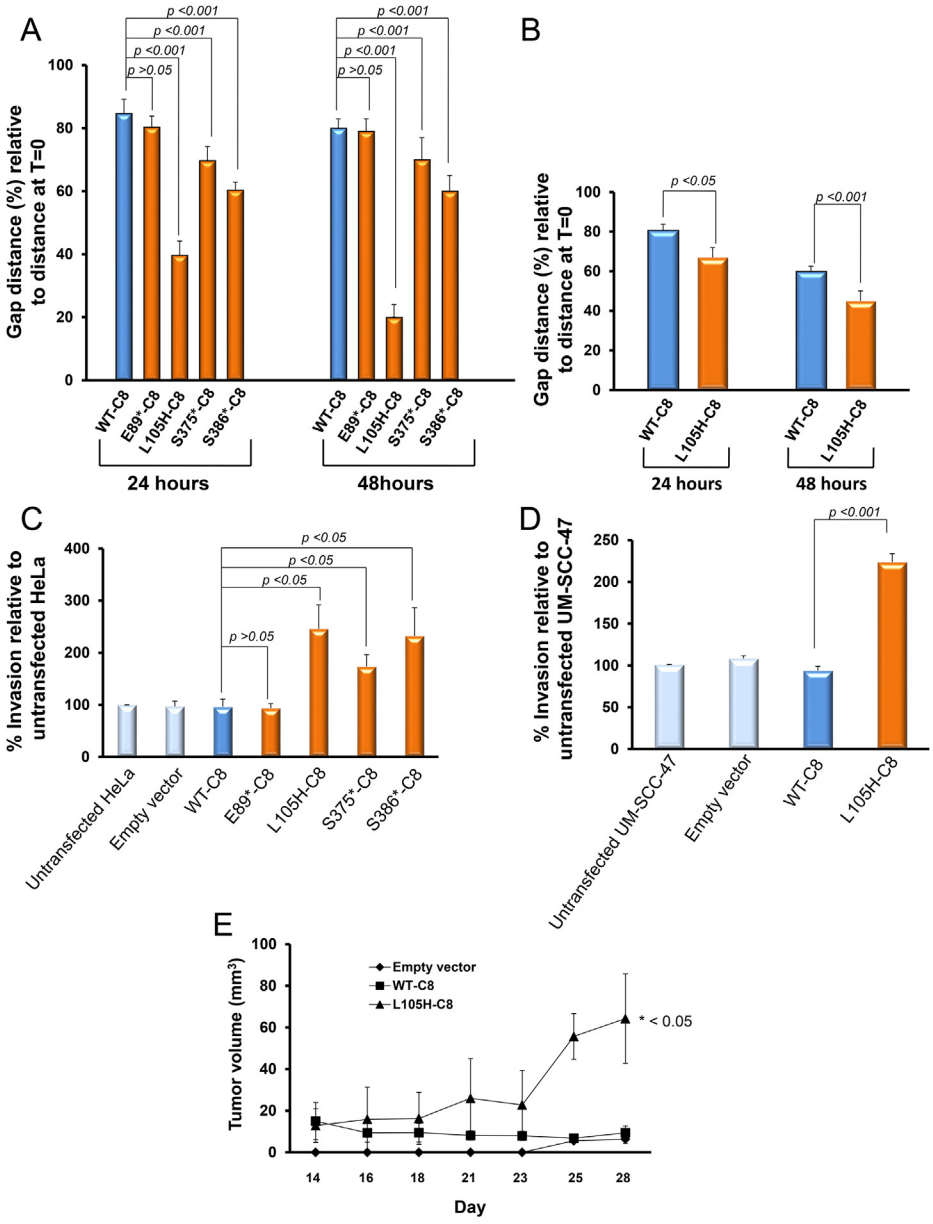

Figure 4 – Procaspase-8 mutant proteins promote migration, invasion, and tumor growth. (A) HeLa cells expressing the indicated proteins were analyzed in migration scratch assays. Gap distances measured after 24 and 48 h were compared with gap distances at $T = 0$ h. Columns represent the means of values obtained in 3 independent experiments (3 gap distances measured per experiment); error bars represent SEM. (B) UM-SCC-47 cells expressing exogenous wild-type or mutant (L105H) procaspase-8 were analyzed in migration scratch assays. Columns represent means from 3 experiments and error bars the SEM. (C) HeLa cells expressing the indicated exogenous proteins were assessed for invasion through matrigel-coated filters. Invasion relative to that seen in untransfected HeLa cells (set at 100%) was calculated. Columns, means from 3 experiments; error bars, SEM. (D) UM-SCC-47 cells expressing the indicated exogenous proteins were assessed for invasion relative to that seen in untransfected UM-SCC-47. Columns, means from 3 independent experiments, error bars, SEM. (E) Athymic nude mice (5 mice/group) were injected in the left and right flanks with empty vector/UM-SCC-47, WT-C8/UM-SCC-47, or L105H/UM-SCC-47 cells, and tumor growth was measured. Data points represent the mean tumor volume of detectable tumors. On day 28, 2 small tumor nodules (out of 10 injection sites) were detected in empty vector/UM-SCC-47 mice, 8 small tumors were detected in WT-C8/UM-SCC-47 mice, and 3 large tumors were detected in L105H-C8/UM-SCC-47 mice. Error bars represent standard deviations.

Recent studies by Dickens et al. (2012) and Schleich et al. (2012) have determined that the levels of procaspase-8 present in the activated DISC greatly exceed those of FADD. This has led to the proposal of a "death effector domain chain" model for caspase-8 activation (Dickens et al., 2012; Schleich et al., 2012). In this model, the DED domain of FADD acts to recruit the DEDa present in the prodomain of procaspase-8. The free DEDb domain of procaspase-8 then recruits the DEDa domain of another procaspase-8 molecule, and elongated chains of recruited procaspase-8 molecules begin to form.

The occurrence of procaspase-8 dimers within these elongated chains results in autoactivation. Mutational analysis has further determined that residues F122 and L123 in DEDb are essential for recruiting the DEDa of another procaspase-8 molecule, and, hence, chain elongation (Dickens et al., 2012). The E89* procaspase-8 truncation mutation evaluated in our experiments lacks the DEDb domain and critical F122/L123 residues, and would be predicted to act as a chain terminator. More extensive sequencing of HNSCC tumors by the TCGA has subsequently identified two additional procaspase-8 truncation mutations lacking the DEDb domain, Arg68* and Q97* mutations (Cerami et al., 2012), which also are likely to act as chain terminators. By contrast, the S375* and S386* truncation mutants we analyzed retain both DED domains, but may inhibit caspase-8 activation through formation of nonfunctional dimers within the elongated chains. The mechanism whereby the L105H missense mutation inhibits caspase-8 activation is unclear. It is notable, however, that multiple missense mutations scattered throughout the procaspase-8 sequence have now been identified by the TCGA (Cerami et al., 2012). Whether these missense mutations exhibit a common mechanism of action, or similarly impact chain elongation, remains to be determined.

The ability of wild-type procaspase-8 to promote motility and migration has been attributed to Src-mediated phosphorylation of Y380 located in the linker region between the large and small subunits (Barbero et al., 2008; Senft et al., 2007; Stupack et al., 2006). The Y380 residue is retained in the L105H and S386* mutants which exhibited enhanced migration and invasion relative to the wild-type procaspase-8 protein. By contrast, the E89* mutant lacks this tyrosine residue, and was the only mutant which did not promote enhanced migration or invasion. Interestingly, the S375* mutant also lacks Y380, but still demonstrated greater migration and invasion than the wild-type procaspase-8 protein. This suggests that phosphorylation of Y380 is not absolutely required for the migration- and invasion-promoting properties of the procaspase-8 mutants.

While it is unknown why fewer detectable tumors were seen following injection of L105H mutant-expressing cells, as compared to injection of wild-type-expressing cells, the mutant tumors grew at a markedly accelerated pace. However, the *in vitro* proliferation rates of cells engineered to express either wild-type or mutant procaspase-8 were nearly identical (data not shown). Thus, the enhanced *in vivo* growth of the L105H mutant-expressing tumors is likely due to other factors, which may include the resistance of these tumor cells to death ligands, or the enhanced migratory and invasive properties of the tumor cells. Interestingly, Pickering et al. have identified caspase-8 mutations in seven different HNSCC cell lines (Pickering et al., 2013). Orthotopic tongue tumors generated from these mutant HNSCC cell lines were generally more aggressive than orthotopic tumors generated from HNSCC cell lines expressing only wild-type caspase-8 (Pickering et al., 2013). These findings further support the potential negative consequences of caspase-8 mutation on HNSCC tumorigenesis.

In summary, our findings demonstrate that procaspase-8 mutations identified in primary tumors from HNSCC patients are capable of potently inhibiting activation of death receptor-mediated extrinsic apoptosis pathways. Thus, procaspase-8 mutation is likely to serve as a biomarker for resistance to therapies incorporating death ligands. Future studies aimed at determining the impact of these mutations on responsiveness to chemotherapy drugs is warranted. Moreover, certain of the mutant procaspase-8 proteins act to promote cellular migration and invasion, and may accelerate tumor growth *in vivo*. These findings provide a rationale for investigating procaspase-8 mutations as prognostic indicators of HNSCC progression.

Conflict of interest

The authors declare no conflict of interest.

Acknowledgements

This work was supported by NIH grants R01 CA137260 and P50 CA097190, and the American Cancer Society. This project also used UPCI shared resources supported in part by NIH grant P30 CA047904. The authors thank Vivian Liu for helpful discussions.

Appendix A. Supplementary data

Supplementary data related to this article can be found at http://dx.doi.org/10.1016/j.molonc.2014.03.018

REFERENCES

Agrawal, N., Frederick, M.J., Pickering, C.R., Bettegowda, C., Chang, K., Li, R.J., Fakhry, C., Xie, T.X., Zhang, J., Wang, J., Zhang, N., El-Naggar, A.K., Jasser, S.A., Weinstein, J.N., Trevino, L., Drummond, J.A., Muzny, D.M., Wu, Y., Wood, L.D., Hruban, R.H., Westra, W.H., Koch, W.M., Califano, J.A., Gibbs, R.A., Sidransky, D., Vogelstein, B., Velculescu, V.E., Papadopoulos, N., Wheeler, D.A., Kinzler, K.W., Myers, J.N., 2011. Exome sequencing of head and neck squamous cell carcinoma reveals inactivating mutations in NOTCH1. Science 333, 1154–1157.

Ando, M., Kawazu, M., Ueno, T., Fukumura, K., Yamato, A., Soda, M., Yamashita, Y., Choi, Y.L., Yamasoba, T., Mano, H., 2013. Cancer-associated missense mutations of caspase-8 activate nuclear factor-kappaB signaling. Cancer Sci. 104, 1002–1008.

Barbero, S., Barila, D., Mielgo, A., Stagni, V., Clair, K., Stupack, D., 2008. Identification of a critical tyrosine residue in caspase 8 that promotes cell migration. J. Biol. Chem. 283, 13031–13034.

Bonner, J.A., Harari, P.M., Giralt, J., Cohen, R.B., Jones, C.U., Sur, R.K., Raben, D., Baselga, J., Spencer, S.A., Zhu, J., Youssoufian, H., Rowinsky, E.K., Ang, K.K., 2010. Radiotherapy plus cetuximab for locoregionally advanced head and neck cancer: 5-year survival data from a phase 3 randomised trial, and relation between cetuximab-induced rash and survival. Lancet Oncol. 11, 21–28.

Cerami, E., Gao, J., Dogrusoz, U., Gross, B.E., Sumer, S.O., Aksoy, B.A., Jacobsen, A., Byrne, C.J., Heuer, M.L., Larsson, E.,

Antipin, Y., Reva, B., Goldberg, A.P., Sander, C., Schultz, N., 2012. The cBio cancer genomics portal: an open platform for exploring multidimensional cancer genomics data. Cancer discov. 2, 401–404.
Chaudhary, P.M., Eby, M.T., Jasmin, A., Kumar, A., Liu, L., Hood, L., 2000. Activation of the NF-kappaB pathway by caspase 8 and its homologs. Oncogene 19, 4451–4460.
Degterev, A., Boyce, M., Yuan, J., 2003. A decade of caspases. Oncogene 22, 8543–8567.
Dickens, L.S., Boyd, R.S., Jukes-Jones, R., Hughes, M.A., Robinson, G.L., Fairall, L., Schwabe, J.W., Cain, K., Macfarlane, M., 2012. A death effector domain chain DISC model reveals a crucial role for caspase-8 chain assembly in mediating apoptotic cell death. Mol. Cell. 47, 291–305.
Finlay, D., Vuori, K., 2007. Novel noncatalytic role for caspase-8 in promoting SRC-mediated adhesion and Erk signaling in neuroblastoma cells. Cancer Res. 67, 11704–11711.
Frisch, S.M., 2008. Caspase-8: fly or die. Cancer Res. 68, 4491–4493.
Fulda, S., 2009. Caspase-8 in cancer biology and therapy. Cancer Lett. 281, 128–133.
Fung, C., Grandis, J.R., 2010. Emerging drugs to treat squamous cell carcinomas of the head and neck. Expert Opin. Emerg. Drugs 15, 355–373.
Helfer, B., Boswell, B.C., Finlay, D., Cipres, A., Vuori, K., Bong Kang, T., Wallach, D., Dorfleutner, A., Lahti, J.M., Flynn, D.C., Frisch, S.M., 2006. Caspase-8 promotes cell motility and calpain activity under nonapoptotic conditions. Cancer Res. 66, 4273–4278.
Hou, W., Han, J., Lu, C., Goldstein, L.A., Rabinowich, H., 2010. Autophagic degradation of active caspase-8: a crosstalk mechanism between autophagy and apoptosis. Autophagy 6, 891–900.
Irmler, M., Thome, M., Hahne, M., Schneider, P., Hofmann, K., Steiner, V., Bodmer, J.L., Schroter, M., Burns, K., Mattmann, C., Rimoldi, D., French, L.E., Tschopp, J., 1997. Inhibition of death receptor signals by cellular FLIP. Nature 388, 190–195.
Jemal, A., Siegel, R., Ward, E., Hao, Y., Xu, J., Thun, M.J., 2009. Cancer statistics, 2009. CA Cancer J. Clin. 59, 225–249.
Kim, H.S., Lee, J.W., Soung, Y.H., Park, W.S., Kim, S.Y., Lee, J.H., Park, J.Y., Cho, Y.G., Kim, C.J., Jeong, S.W., Nam, S.W., Kim, S.H., Lee, J.Y., Yoo, N.J., Lee, S.H., 2003. Inactivating mutations of caspase-8 gene in colorectal carcinomas. Gastroenterology 125, 708–715.
Li, C., Johnson, D.E., 2013. Liberation of functional p53 by proteasome inhibition in human papilloma virus-positive head and neck squamous cell carcinoma cells promotes apoptosis and cell cycle arrest. Cell Cycle 12, 923–934.
Lin, C.J., Grandis, J.R., Carey, T.E., Gollin, S.M., Whiteside, T.L., Koch, W.M., Ferris, R.L., Lai, S.Y., 2007. Head and neck squamous cell carcinoma cell lines: established models and rationale for selection. Head Neck 29, 163–188.
Mandruzzato, S., Brasseur, F., Andry, G., Boon, T., van der Bruggen, P., 1997. A CASP-8 mutation recognized by cytolytic T lymphocytes on a human head and neck carcinoma. J. Exp. Med. 186, 785–793.
Martin, D.A., Siegel, R.M., Zheng, L., Lenardo, M.J., 1998. Membrane oligomerization and cleavage activates the caspase-8 (FLICE/MACHalpha1) death signal. J. Biol. Chem. 273, 4345–4349.
Mehanna, H., Paleri, V., West, C.M., Nutting, C., 2010. Head and neck cancer–Part 1: epidemiology, presentation, and prevention. Bmj 341, c4684.
Muzio, M., Stockwell, B.R., Stennicke, H.R., Salvesen, G.S., Dixit, V.M., 1998. An induced proximity model for caspase-8 activation. J. Biol. Chem. 273, 2926–2930.
Oberst, A., Dillon, C.P., Weinlich, R., McCormick, L.L., Fitzgerald, P., Pop, C., Hakem, R., Salvesen, G.S., Green, D.R., 2011. Catalytic activity of the caspase-8-FLIP(L) complex inhibits RIPK3-dependent necrosis. Nature 471, 363–367.
Pickering, C.R., Zhang, J., Yoo, S.Y., Bengtsson, L., Moorthy, S., Neskey, D.M., Zhao, M., Ortega Alves, M.V., Chang, K., Drummond, J., Cortez, E., Xie, T.X., Zhang, D., Chung, W., Issa, J.P., Zweidler-McKay, P.A., Wu, X., El-Naggar, A.K., Weinstein, J.N., Wang, J., Muzny, D.M., Gibbs, R.A., Wheeler, D.A., Myers, J.N., Frederick, M.J., 2013. Integrative genomic characterization of oral squamous cell carcinoma identifies frequent somatic drivers. Cancer discov. 3, 770–781.
Schleich, K., Warnken, U., Fricker, N., Ozturk, S., Richter, P., Kammerer, K., Schnolzer, M., Krammer, P.H., Lavrik, I.N., 2012. Stoichiometry of the CD95 death-inducing signaling complex: experimental and modeling evidence for a death effector domain chain model. Mol. Cell. 47, 306–319.
Senft, J., Helfer, B., Frisch, S.M., 2007. Caspase-8 interacts with the p85 subunit of phosphatidylinositol 3-kinase to regulate cell adhesion and motility. Cancer Res. 67, 11505–11509.
Soung, Y.H., Lee, J.W., Kim, S.Y., Jang, J., Park, Y.G., Park, W.S., Nam, S.W., Lee, J.Y., Yoo, N.J., Lee, S.H., 2005a. CASPASE-8 gene is inactivated by somatic mutations in gastric carcinomas. Cancer Res. 65, 815–821.
Soung, Y.H., Lee, J.W., Kim, S.Y., Sung, Y.J., Park, W.S., Nam, S.W., Kim, S.H., Lee, J.Y., Yoo, N.J., Lee, S.H., 2005b. Caspase-8 gene is frequently inactivated by the frameshift somatic mutation 1225_1226delTG in hepatocellular carcinomas. Oncogene 24, 141–147.
Stransky, N., Egloff, A.M., Tward, A.D., Kostic, A.D., Cibulskis, K., Sivachenko, A., Kryukov, G.V., Lawrence, M.S., Sougnez, C., McKenna, A., Shefler, E., Ramos, A.H., Stojanov, P., Carter, S.L., Voet, D., Cortes, M.L., Auclair, D., Berger, M.F., Saksena, G., Guiducci, C., Onofrio, R.C., Parkin, M., Romkes, M., Weissfeld, J.L., Seethala, R.R., Wang, L., Rangel-Escareno, C., Fernandez-Lopez, J.C., Hidalgo-Miranda, A., Melendez-Zajgla, J., Winckler, W., Ardlie, K., Gabriel, S.B., Meyerson, M., Lander, E.S., Getz, G., Golub, T.R., Garraway, L.A., Grandis, J.R., 2011. The mutational landscape of head and neck squamous cell carcinoma. Science 333, 1157–1160.
Stupack, D.G., Teitz, T., Potter, M.D., Mikolon, D., Houghton, P.J., Kidd, V.J., Lahti, J.M., Cheresh, D.A., 2006. Potentiation of neuroblastoma metastasis by loss of caspase-8. Nature 439, 95–99.
Torres, V.A., Mielgo, A., Barbero, S., Hsiao, R., Wilkins, J.A., Stupack, D.G., 2010. Rab5 mediates caspase-8-promoted cell motility and metastasis. Mol. Biol. Cell. 21, 369–376.
Yang, X., Chang, H.Y., Baltimore, D., 1998. Autoproteolytic activation of pro-caspases by oligomerization. Mol. Cell. 1, 319–325.
Zhao, Y., Sui, X., Ren, H., 2010. From procaspase-8 to caspase-8: revisiting structural functions of caspase-8. J. Cell Physiol. 225, 316–320.